# Analysis of numerical solution to 2D Laplace equation on a rectangular electric field plate assembly

Nikolaos Koukoulekidis
CID: 00950301

December 19, 2016

**Abstract**

The Jacobi and Successive Over-Relaxation (SOR) methods were used to solve the 2D Laplace equation on a square grid containing fixed square potential. Their convergence speed were found proportional to the $scale^2$ and $scale$ respectively. The effect of the square width on potential field was examined. SOR was used to model an experimental parallel plate array (figure 1) [1]. The homogeneity of the electric field was found to drop exponentially near the edges of the plates and its response to plate impurities was examined.

## 1 Introduction

Most experiments that generate electric fields involve complicated electric plate arrays and thus the generated fields cannot be modelled analytically. The general 3D Poisson equation that governs these systems is an elliptic partial differential equation that usually satisfies Dirichlet boundary conditions. Therefore, it can be solved numerically on a spatial grid.

The electron electric dipole moment (EDM) experiment conducted at the Centre for Cold Matter at Imperial College London [1] uses an array of long parallel aluminium plates. The aim is to generate a homogeneous electric field between them through which particles can travel along a straight line [2]. A simplified model of the system is illustrated in figure (1). The plates are parallel to each other and are held in a vacuum. Therefore, the problem of obtaining a numerical solution for the electric potential $\phi$ reduces to solving the 2D Laplace equation.

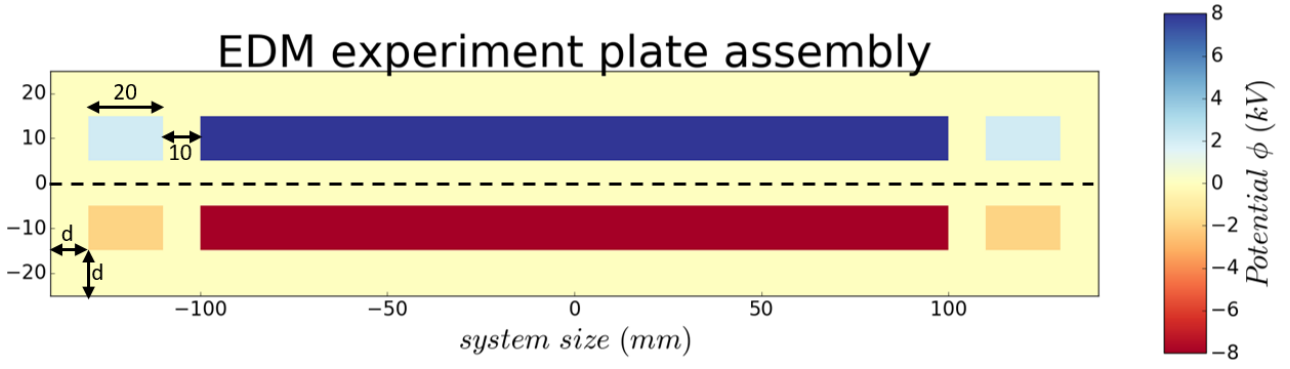


Figure 1: Simplified electric field plate assembly investigated in this report. It consists of two big plates, $200mm \times 10mm$ at $\pm 8kV$ and four small plates, $20mm \times 10mm$ at $\pm 2kV$ enclosed in a rectangular vacuum chamber [3] with walls at a distance $d$ from the plates. Here, $d = 10mm$. The dashed line indicates the particle path. The system is symmetric along the path and its bisecting line.

The aim of this report is to investigate the solution to the 2D Laplace equation applied on a simplified square grid with a square electric plate in the middle and implementing the results on the EDM

experiment plate assembly of figure (1). The Jacobi and Successive Over-Relaxation (SOR) methods are used to obtain solutions and studied in terms of efficiency. Criteria are developed for assessing convergence to the solution and reflecting important physical features of the system. In the context of the EDM experiment, the homogeneity of the electric field along the particle path is estimated as well as its dependence on small deformations of the plates.

## 2 Theory of numerical methods

Initial investigations involve the electric potential of a simple square grid, as in figure (2). This can be thought of as the cross section of an infinitely long square coaxial cable of fixed potential inside a square vacuum tube. The Laplace equation of such a system, including the EDM experiment assembly, is

$$\nabla^2\phi = 0 \tag{1}$$

where $\nabla^2 \equiv \frac{\partial^2}{\partial x^2} + \frac{\partial^2}{\partial y^2}$ in this case.

To solve this equation, the system is represented by a grid with a scale parameter. In figure (2), the scale is 100 grid points per $2cm$ which is taken as the unit length of the system. Then, it is possible to iterate over the system until convergence by applying the Jacobi pictorial operator

$$\boldsymbol{J} = \frac{1}{4}\begin{bmatrix} & 1 & \\ 1 & 0 & 1 \\ & 1 & \end{bmatrix}, \tag{2}$$

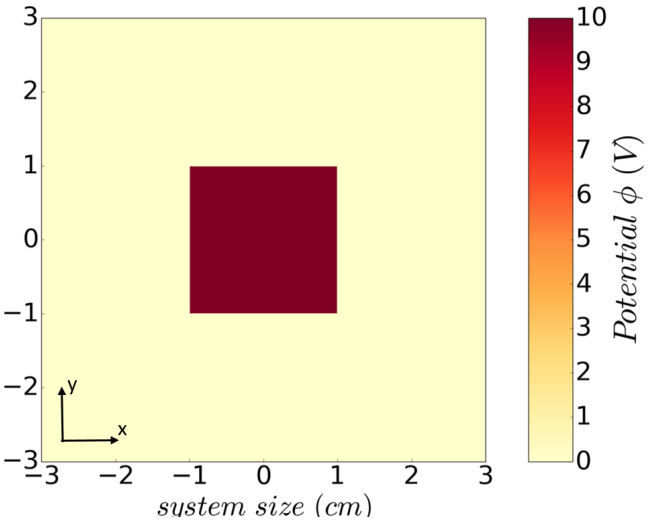


Figure 2: Simple 2D symmetric square grid with a square plate in the middle at potential $\phi = 10\ V$. The square boundaries are grounded.

such that $\phi_{i,j}^{(n+1)} = \boldsymbol{J}\phi_{i,j}^{(n)}$. This is essentially a temporal update ($n \to n+1$) which is done by averaging over the four nearest neighbours of a grid point at position $(x, y) = (i, j)$. The neighbours may be the boundaries of the system, including the cable. This is the Jacobi method which is consistent, stable and second-order accurate in this case. The new grid points are not used in the calculations of the current update, making the method slow compared to SOR.

For this reason, SOR is used throughout the analysis. It is a modification of the Jacobi method, such that

$$\phi_{i,j}^{(n+1)} = (1-\omega)\phi_{i,j}^{(n)} + \omega\left[\boldsymbol{J}\psi_{i,j}^{(n+\frac{1}{2})}\right], \tag{3}$$

where $\omega$ is the relaxation parameter and $\psi_{i,j}^{(n+\frac{1}{2})}$ symbolically represents the next component to be updated. SOR is a forward scheme meaning that all previous components need to have been computed before averaging around $\psi_{i,j}^{(n+\frac{1}{2})}$. Therefore, unlike the Jacobi method, the averaging includes neighbours from both updates $n$ and $n+1$, explaining the superscript.

The relaxation parameter can be tuned to yield faster algorithms. It is shown in the Appendix that through numerical coarse graining on small system scales the optimal value is close to

$$\omega_{opt} = \frac{2}{1 + \frac{C}{r \times scale}}, \tag{4}$$

where $r$ is the ratio of the two dimensions of the system, thus 1 for the square grid, and $C = 2.0$ and 5.5 for the square cable and the EDM experiment assemblies respectively. These scale dependent values are extrapolated to finer resolutions [4].

## 3 Method

Determining satisfactory criteria for solution convergence is necessary to save computational time. The general principle used in the investigation was to claim convergence when the temporal electric potential spread was negligible compared to the spatial spread $\epsilon$ on the grid. The spatial spread is a measure of the potential difference between neighbouring grid points, while the temporal spread is the norm $||\boldsymbol{\phi}^{(n+1)} - \boldsymbol{\phi}^{(n)}||$, where $\boldsymbol{\phi}$ is the vector of grid points at given update. When further iterations decrease the temporal spread below $\beta\epsilon, \beta < 0.05$, where $\beta$ is an accuracy coefficient, further iterations affect the spatial convergence of the system negligibly and are thus stopped. In practice, SOR is so fast that important calculations are performed to floating point precision in the temporal spread ($\beta \approx 10^{-11}$). These include calculations of the electric field, when it is important to minimise random noise to examine homogeneity.

The spatial spread is a good criterion for convergence because it is bounded below by the scale of the system and thus temporal convergence is well defined. This is illustrated in figure (3) and raises the question of what is the optimal scale to reflect the physical nature of the system. It can be seen in the figure, that the spatial spread cannot be decreased arbitrarily by enhancing accuracy at a constant scale, as expected. The scale ultimately limits the information that can be gained from the system.

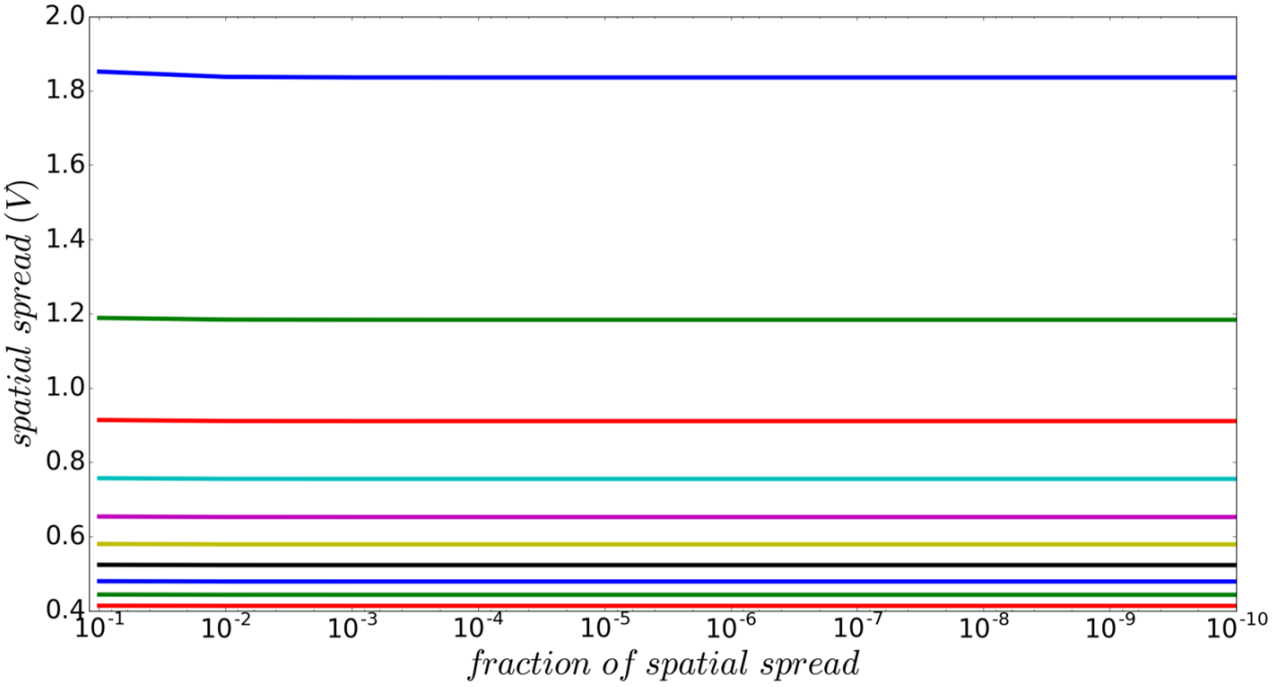


Figure 3: Spatial spread against accuracy factor $\beta$ for the square grid. The tube to cable width ratio is 3. The scale of the system is varied linearly between 10 (top line), $20, 30, \ldots$ and 100 (bottom line).

Trivially, it can be said that the minimum scale for the EDM experiment is 1 grid point per $10mm$ which just resolves the plates and the gaps between them. Of course, it is desired to increase the scale and smooth out the features. According to figure (3), if we want to resolve the potential at a spread of $1.2V$, a scale equal to 20 grid points per unit length is needed.

In order to measure electric field homogeneity between two parallel plates in the EDM experiment, the fractional deviation of the electric field magnitude along the particle path was compared to its value

exactly at the midpoint between the two plates. The magnitude was approximated with a second and a fourth order accurate scheme for the derivatives along the $x$ and $y$ directions respectively, expecting a far more significant contribution of the $y$-component since it is perpendicular to the path.

# 4 Results and Discussion

### Square Cable

The accuracy factor $\beta$ is set to 0.05 for this system, because there is no observable difference at lower factors, as seen clearly in figure (3). One solved (converged) system is illustrated in figure (4) for the ratio of tube width over cable width equal to 3. The potential smoothens out to become more circular away from the cable, but it is forced to drop to 0 at the boundaries of the tube, which does not allow the potential to resemble point-charge-like behaviour.

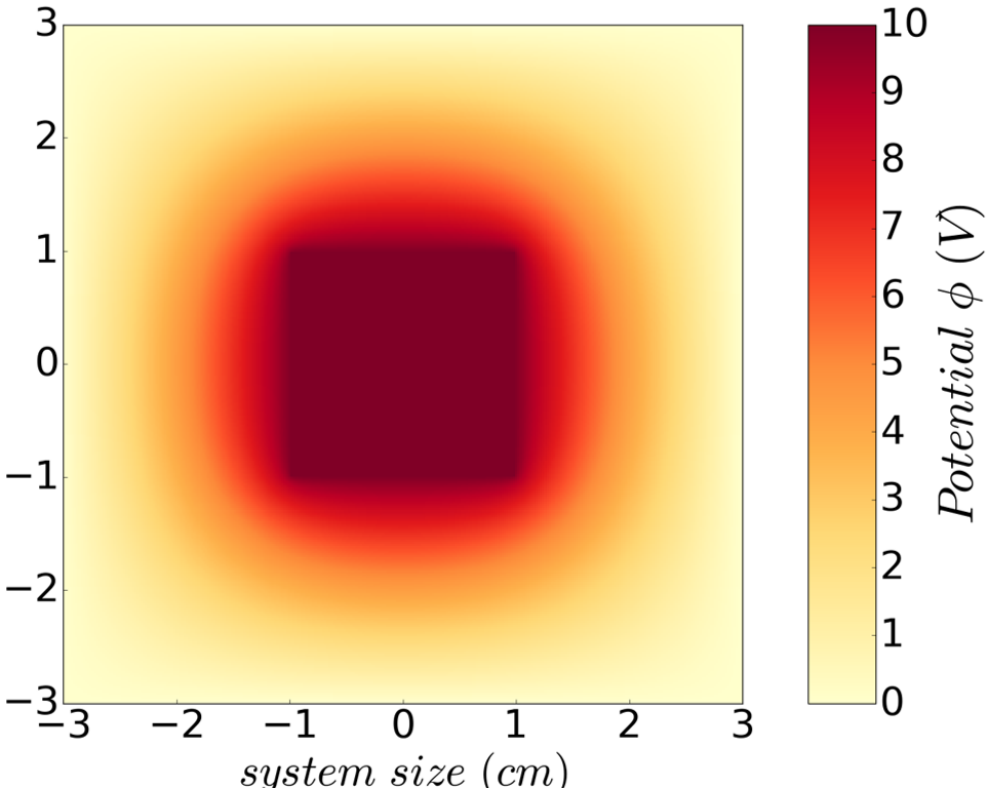


Figure 4: Solved square cable system for tube to cable width ratio equal to 3.

The characteristic parameters of this system are its scale and the tube to cable width ratio, so both are examined more closely. The former parameter is interesting computationally, while the latter gives physical insight into the system.

As discussed earlier, the larger the scale, the more information there is to be gained from the system. Larger scales, however, compromise efficiency. Figure (5) represents the scale-depending behaviour of the computational efficiency required to solve the system with the Jacobi method.

The number of updates looks proportional to the square of the scale, which is an important feature. This is to be expected in a 2D system that is solved with the Jacobi method. The volume of the system scales with the square of the system scale and the Jacobi method is neither forward nor backward. Only once the pictorial operator has scanned the whole volume, the newly updated grid points will be used for further updates. As this is not the case for SOR, we expect a different, more efficient, dependence of updates on the system scale. This is confirmed by figure (6) which illustrates a linear trend with scale, when the optimal relaxation parameter is used at each scale.

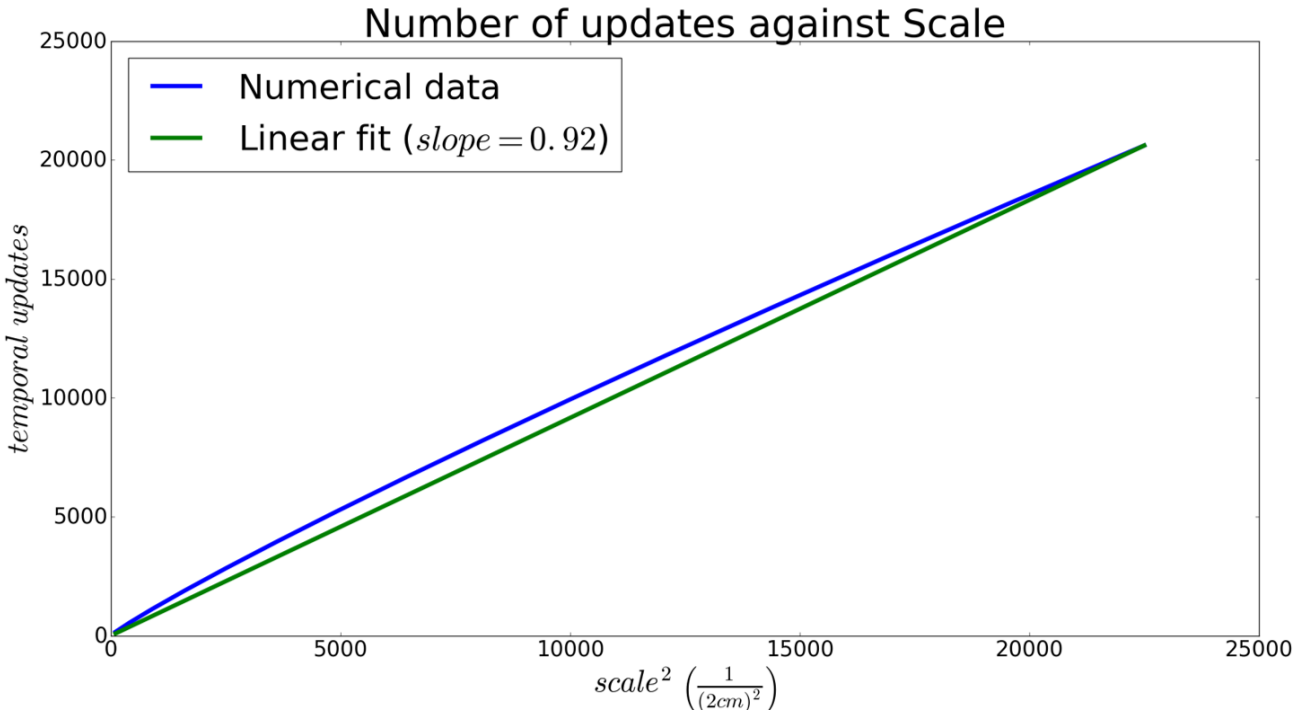


Figure 5: Convergence with Jacobi method. The number of iterations needed for convergence closely follows a parabolic trend with system scale. The plot extends from scale 10 to 150.

The inverse of number of temporal updates can be thought of as the computational speed of the algorithm, while the scale is the inverse of mesh spacing. This leads to equivalently restating the results that the convergence speed scales with the square of the mesh spacing for the Jacobi method and the mesh spacing itself in the SOR method. Of course, strong evidence for the difference in the speed is merely provided by observing that the number of updates in figure (6) does not exceed 1000 which corresponds to a scale of only 33 grid points per unit length for the Jacobi method. The slopes are system dependent and do not reveal much more information than the linearity of the trends.

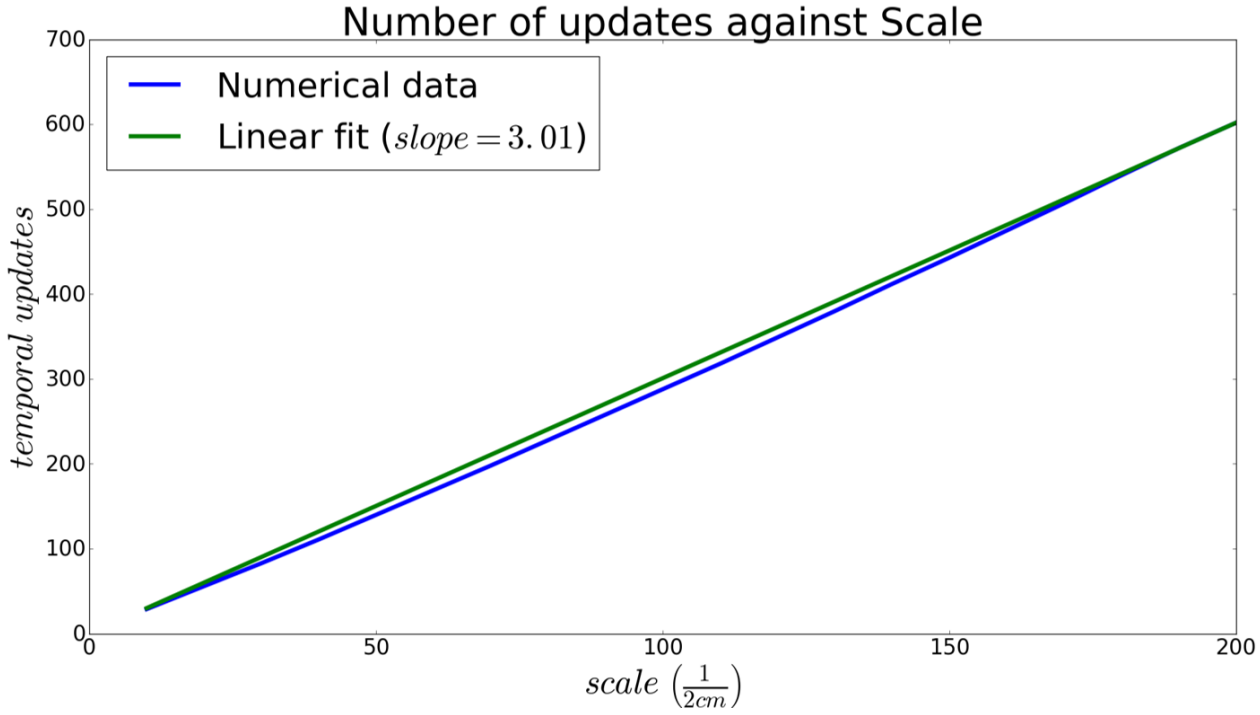


Figure 6: Convergence with SOR method. The number of iterations needed for convergence closely follows a linear trend with system scale. The plot extends from scale 10 to 200.

Moving on to the effect of the tube to cable width ratio on the potential field, figure (7) provides the necessary information to explain it. For ratios close to 1 the two boundaries, the cable and the tube, are very close together and the behaviour of the potential field is linear as is the expactation for two parallel plates. As the ratio becomes larger, the potential field lines tend to drop with a logarithmic or inverse dependence to the radial distance. This approximates the potential field of an infinitely long wire or point charge respectively, which is expected as the cable cross section tends to be very small compared to the tube as the ratio increases. The two functional forms look similar, but do not reflect the true nature of the plot. The important difference is that the potential field must drop to 0 at the boundary and cannot continue decreasing below 0 or asymptotically, which is the case for an infinite wire and a point charge respectively.

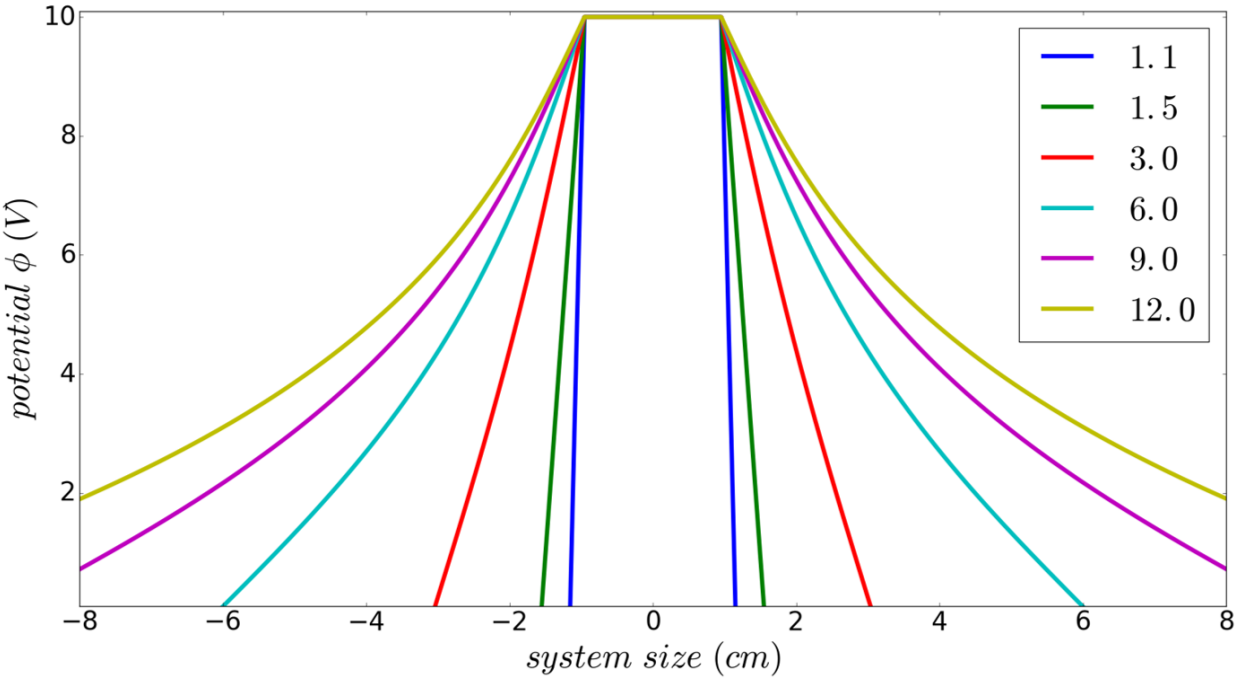


Figure 7: 1D cross section of the system illustrating the potential field behaviour for different tube to cable width ratios as instructed by the legend. The dependence on distance changes from linear for small ratios to logarithmic for big ratios.

This feature also suggests that a small tube distance be used for the EDM experiment. It is beneficial to resemble linear behaviour, which is steeper and therefore it is more difficult for the particle to diverge from its path. In other words, the particle enters from a tube boundary along the designated path and stays on the path more easily, without heading towards a plate, until it reaches close to the plates, for example at $-130mm$ in figure (8), which then direct the motion of the particle.

### EDM assembly

Using all the previous results, the EDM experiment plate assembly can now be simulated. The tube distance from the plates is chosen to be $d = 10mm$ as in figure (1), which is short, as required. The solved system for this tube distance is portrayed in figure (8). The particle trajectory is clearly marked by the 0 potential field between the plates.

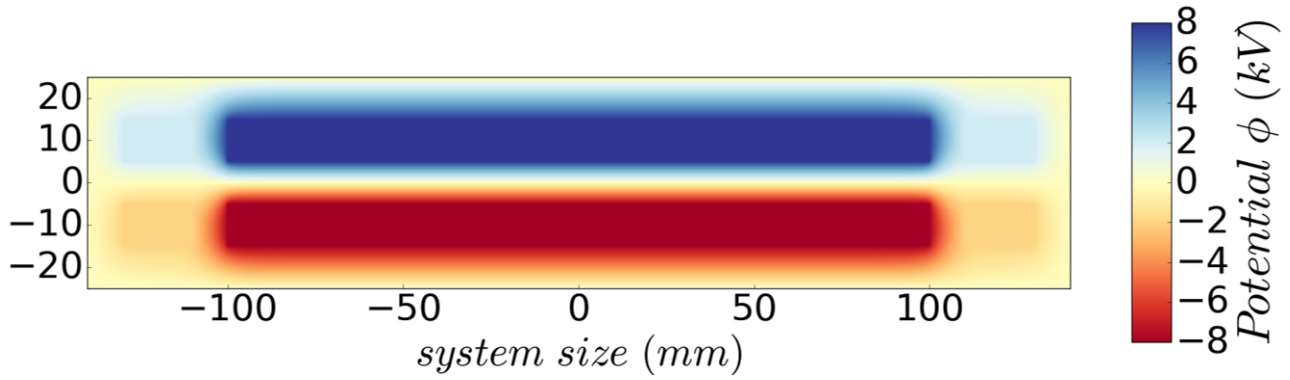


Figure 8: Converged EDM experiment assembly for tube to plate distance $d = 10mm$.

In this system, the most important feature is the homogeneity of the electric field on the trajectory. Figure (9) represents the magnitude of the electric field in the region between the plates. It is four times larger in magnitude between the big plates, than between the small plates, which is expected as the potential is four times larger as well. The $10mm$ region between the big and the small plates see a rapid increase in electric field. It can already be seen from figure (9) that it is hard for the regions between the small plates to remain homogeneous due to their short width and large edge effects.

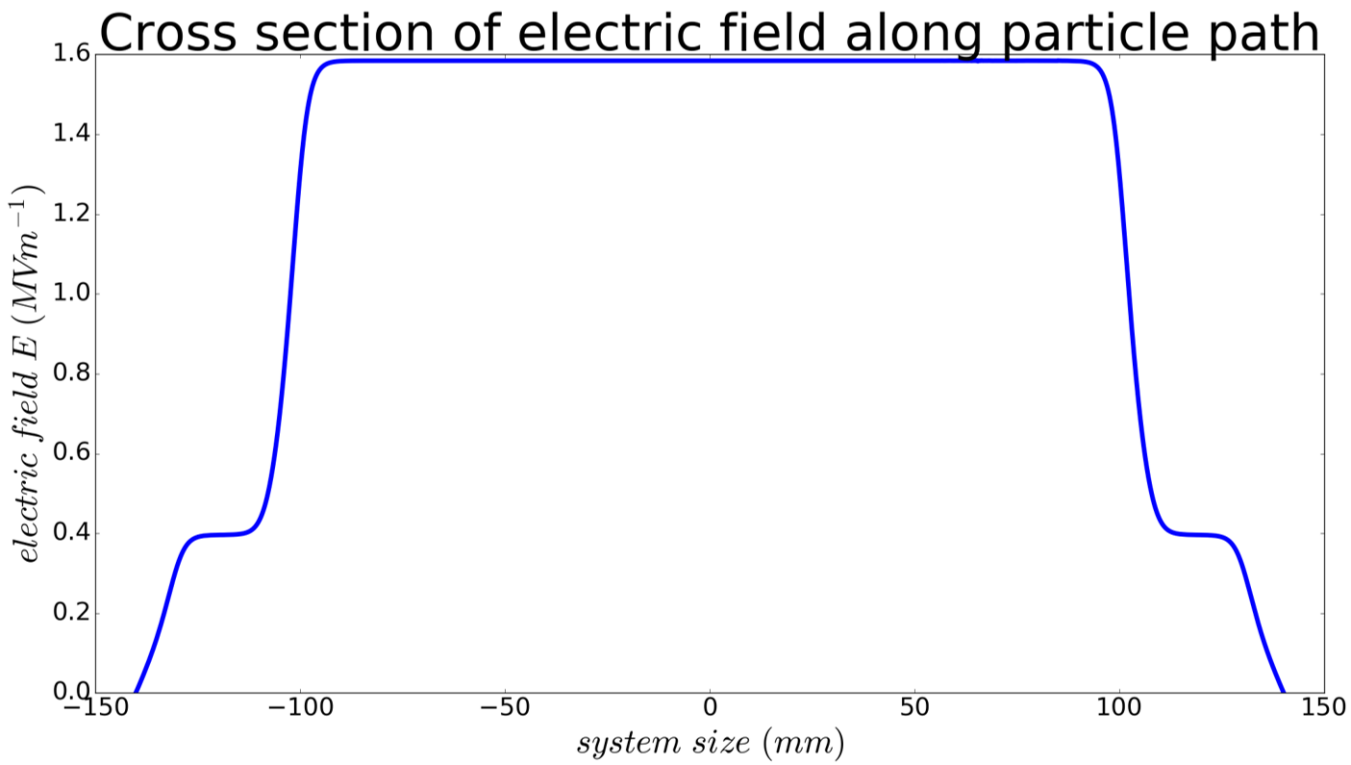


Figure 9: Magnitude of electric field along the particle trajectory

The metric of homogeneity is the fractional deviation of its magnitude as defined in the Methods section. Figure (10) illustrates the change in the neighbourhood of homogeneity of each plate with the homogeneity threshold level.

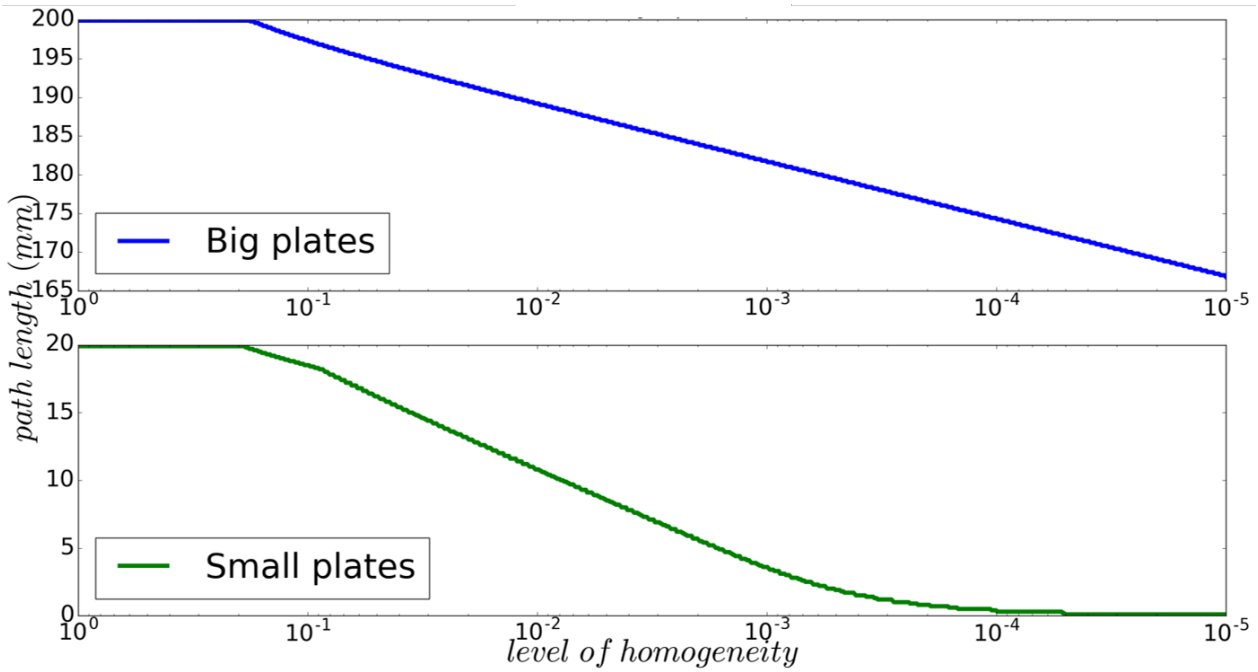


Figure 10: The radius of homogeneity drops exponentially with the homogeneity threshold level of the electric field magnitude on the particle trajectory.

The exponential drop is very clear for the big plates. At a level of 0.001% (= $10^{-5}$ in the graph) homogeneity the neighbourhood of the homogeneous field has shrunk by about $35mm$. The regions that are first to escape the neighbourhood are symmetrically at the edges of the plate where edge effects are observable. The small plates have significantly lower potential and more importantly shorter width and thus the edge effects are more dominant. Hence, they are not homogeneous at all at the level of 0.001%. In fact, at very low radii of homogeneity, the trend loses its linearity as the radius drops to 0. This is because the edge effects are significantly suppressed at the middle of the plate and it is more difficult for the central region between the plates to escape the neighbourhood of homogeneity. However, homogeneity can still be predicted from the linear trend at a level of 0.1%.

Homogeneity is explored further by adding small impurities on the plates. The impurities are of scale $100\mu m$, which is 100 times smaller than the unit length of the EDM experiment ($10mm$) and thus require a scale of at least 100 to be captured by the mesh spacing of the model. Figure (5) matches scale 100 to around 10000 updates for the square system and therefore more updates for the EDM experiment which has a larger unit grid. In fact the Jacobi method yield 4000 updates for scale 50 in the EDM case, thus doubling the scale results in 16000 updates. However, simulations were run with the SOR method since it is significantly faster. Impurities were added at various parts of all the plates. They had a fixed potential of 0 if they were modelled as insulators or of the value the plate they were on has. Figure (11) shows the most profound effect on the electric field when an impurity is added on the top central plate facing the path. The system does not remain symmetric along the $x$ axis and therefore the $y$ component of the electric field is distorted. In the case of a conducting impurity, referred as dust on the plot, the component is elongated towards the impurity, while the opposite happens when the dust is an insulator. After convergence, a conducting impurity is a lot closer to that grid point's value if there was no impurity because it is placed directly near a plate. The opposite is true again for an insulating impurity, which explains the rapid and wider decrease in the magnitude of the electric field in that region compared to the small rise observed when conducting dust is added instead.

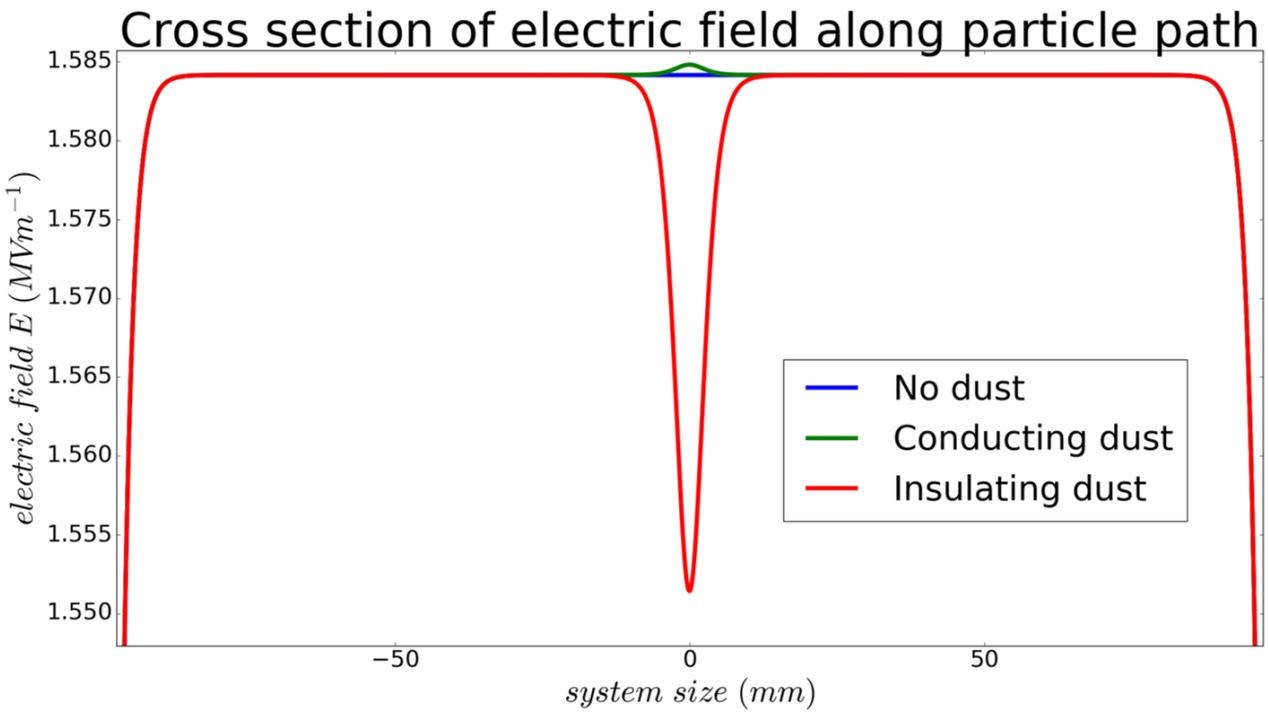


Figure 11: Electric field with an impurity of size $100\mu m$ added at the centre of the middle plate facing the particle trajectory. Insulating impurities have a more significant effect than conducting impurities.

## 5 Conclusion

The aim of the project was to investigate numerical solutions to the 2D Laplace equation and apply them on a plate assembly to examine the physical properties of the system. The Jacobi and SOR iterative methods were used and the latter was found to converge significantly faster to a solution for the potential field. A simplified version of the EDM experiment plate assembly at Imperial College London was analysed with respect to the size and scale of the system and most importantly the homogeneity of the electric field that drives the particles through the system.

The walls of the EDM experiment assembly were found to be optimally positioned close to the plates, while impurities of the plates had more significant impact to the field homogeneity when they had insulating rather than conducting behaviour. Most of the potential field analysis was performed on a simplified square grid, suggesting that the results are generally transferable between systems. The project could be extended to include a 3D model of the assembly which would give deeper insight into the appropriate size of the chamber which encloses the assembly. It could also include analyses of the quality of electric field reversal when particles are crossing which would capture a major complication of the experiment, but would be computationally more demanding.

## Appendix

The SOR parameter $\omega$ can only take values between 0 and 2, so that the algorithm converges [5]. Expecting a result of the form of equation (4) [4], an analysis is performed on coarse systems so that it is extrapolated to finer scales.

The minimum number of updates required for convergence can be estimated for a system of given scale, by varying the relaxation parameter. Figure (12) shows that indeed as the scale increases, the the optimal value of the parameter increases as well. This figure shows analysis performed on the square grid.

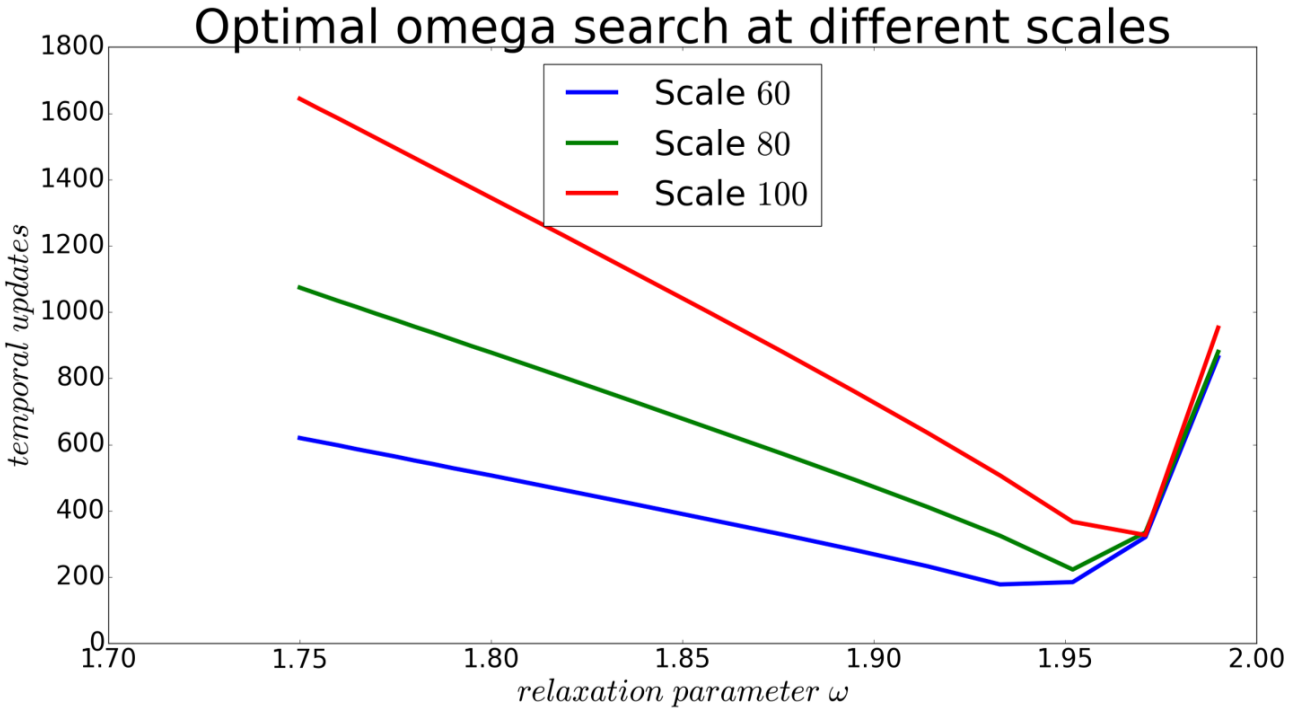


Figure 12: As scale increases the minimum required number of updates for convergence shifts to larger $\omega$ values.

By varying the scale, the trend of optimal $\omega$ is examined in figures (13) and (14) for the square grid and the EDM experiment respectively. By trial and error, a suitable value of the constant $C$ in equation (4) was estimated for both systems to best fit the numerical data acquired. The trends of the fitted curves were extrapolated to systems of a general scale.

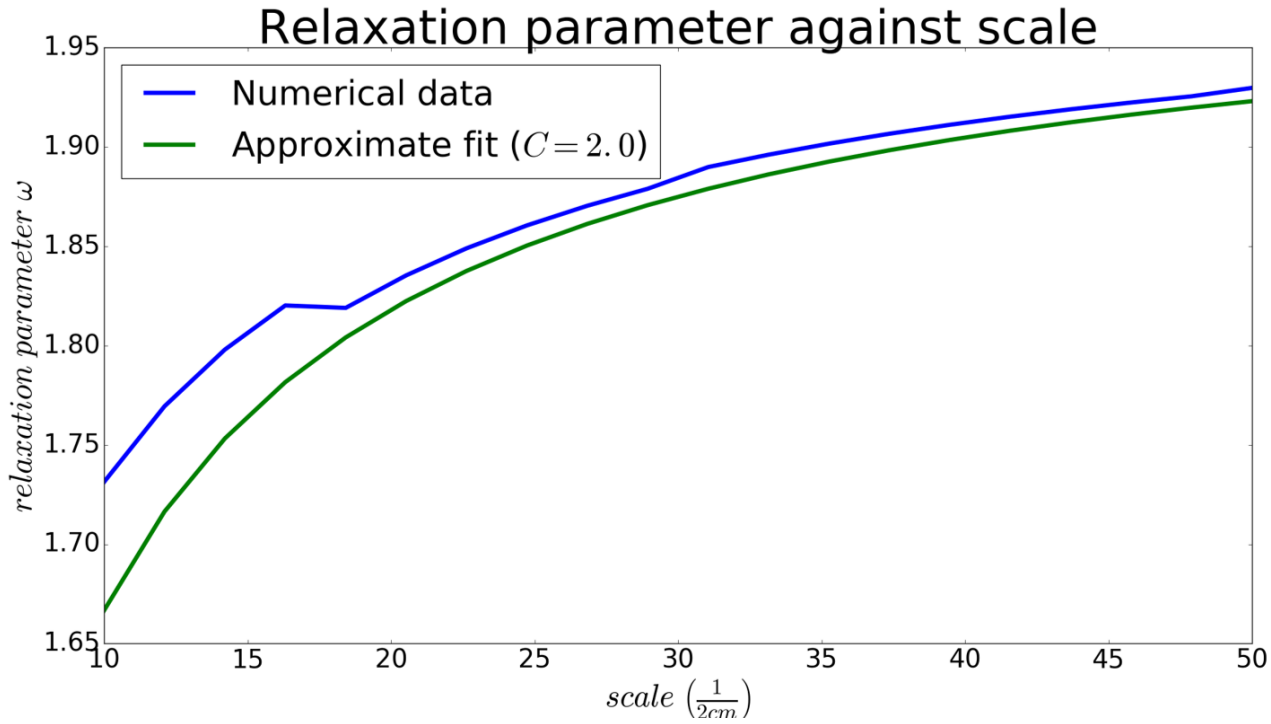


Figure 13: The numerical estimations fit well with the theoretical expectation for the square grid.

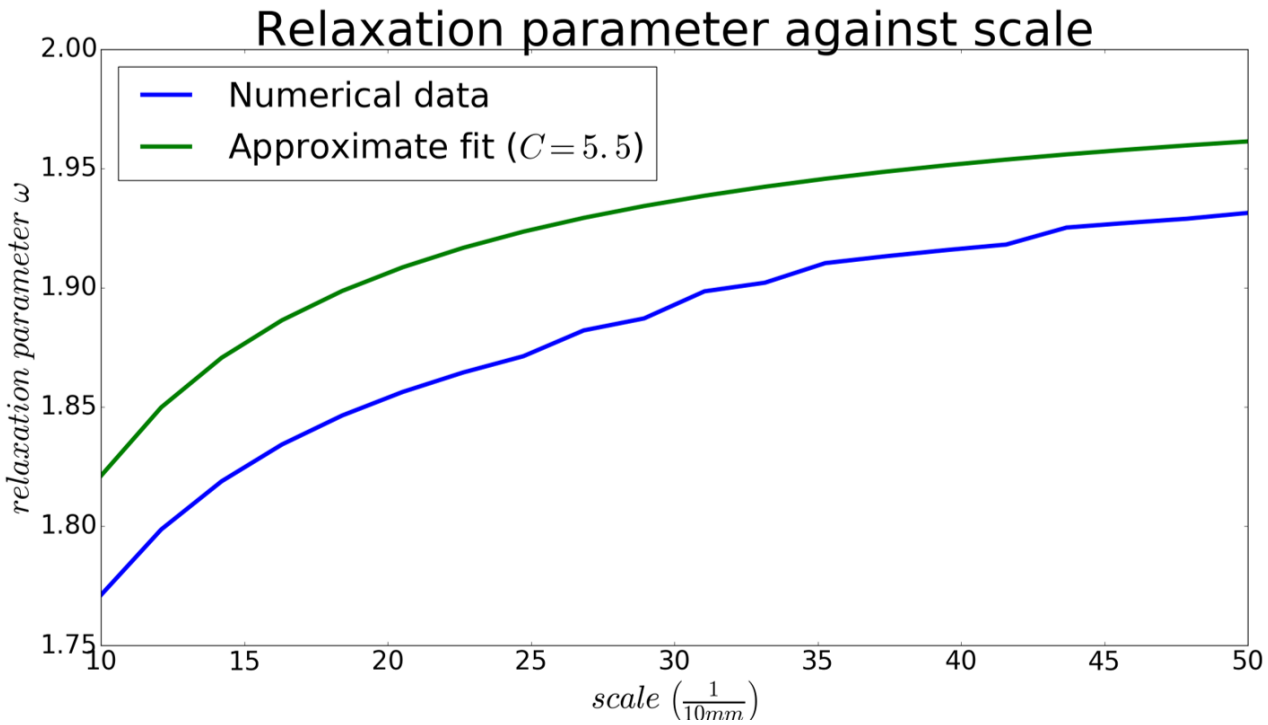


Figure 14: The numerical estimations fit well with the theoretical expectation for the EDM experiment grid.

## References


[1] Imperial College London. (2016) *Electron edm.* Available from here [Accessed 18th December 2016]

[2] Ashworth, H. (2008) *Towards an improved measurement of the electron electric dipole moment.* PhD thesis. University of London.

[3] Hudson, J. J. (2001) *Measuring the electric dipole moment of the electron with YbF molecules.* PhD thesis. University of Sussex.

[4] Saad, Y. (2003) *Iterative Methdos for Sparse Linear Systems.* Society for Industrial and Applied Mathematics.

[5] Hadjidimos, A. (2000) *Successive overrelaxation (SOR) and related methods* . Journal of Computational and Applied Mathematics. 123 (1-2), 177-199


[Words: 2492]